From branched self-assemblies to branched mesoporous silica nanoribbons†

Baozong Li,[a] Yuanli Chen,[a] Huanyu Zhao,[a] Xianfeng Pei,[a] Lifeng Bi,[a] Kenji Hanabusa[b] and Yonggang Yang*[a]

Received (in Cambridge, UK) 14th July 2008, Accepted 28th August 2008
First published as an Advance Article on the web 4th November 2008
DOI: 10.1039/b812016a

Branched left-handed twisted mesoporous silica nanoribbons were prepared *via* a template method.

Recently, branched, hyperbranched, Y- and star-shaped nanoparticles have attracted many researchers, because they can be potentially applied in the fields of electronics and photonics. However, only a few methods have been used to control the branched nanostructures. For example, branched ε-MnO_2 nanostructures were synthesized *via* a hydrothermal method.[1] Hyperbranched PbSe nanowire networks were synthesized *via* a vapor–liquid–solid mechanism.[2] Star-shaped Bi_2S_3 was formed by the splitting crystal growth mechanism.[3] Star-shaped gold nanoparticles were synthesized using a surfactant direct method.[4] Boron nanowire Y-junctions were synthesized in a self-assembled manner by fusing two individual boron nanowires grown inclined toward each other.[5] Multibranched carbon nanotubes were synthesized using flow fluctuation.[6] Y-junction carbon nanotubes were grown by a chemical vapor deposition method using nanochannel alumina as a template.[7]

Low-molecular-weight amphiphiles show a variety of morphologies. Recent results indicated that sol–gel transcription is a powerful method to control inorganic, organic–inorganic hybrid, and organic nanostructures using the self-assemblies of these amphiphiles as templates.[8–13] The morphologies of organic templates can control those of inorganic nanomaterials. Up to now, nanofibers, nanotubes, and mesoporous nanofibers have been prepared. For the preparation of branched nano-silicas through a sol–gel transcription process, branched organic self-assemblies should be selected as templates, at least, branched organic self-assemblies as intermediates can be formed during the sol–gel transcription process. Here we successfully obtained branched mesoporous silica nanostructures through a dynamic templating process. The branched mesoporous silicas have potential to be used as templates to prepare other nanomaterials.

Amphiphile L-**16Phe6PyBr** which is composed of L-phenylalanine was synthesized according to Scheme 1 (ESI †).[12] It can gel THF, benzene, nitrobenzene, 1,4-dioxane, and chlorobenzene. When 10 mg of L-**16Phe6PyBr** were dissolved in 1.0 mL of pure water, a white suspension was obtained. An optical micrograph shows many short ribbons and fibers of μm-size floating in water (Fig. 1a). It is interesting to find that huge branched organic self-assemblies were identified when 10 mg of L-**16Phe6PyBr** were dissolved in 1.0 mL of 1-propanol. According to our previous results,[11,12] branched silica nanostructures are potentially obtained *via* the sol–gel transcription method.

Because it is hard to transfer the morphologies of the self-assemblies of L-**16Phe6PyBr** in pure 1-propanol, the sol–gel transcriptions were carried out in mixtures of water and 1-propanol. A typical synthetic procedure is as follows: compound L-**16Phe6PyBr** (10 mg, 0.016 mmol) was dissolved in a mixture of 0.2 mL of 1-propanol and 0.8 mL of NH_3 aq. (5.0 wt%), then 20 mg (0.096 mmol) of tetraethoxyl orthosilicate (TEOS) were dropped into the suspension under strong stirring at 0 °C. After it turned white at 90 s, stirring was stopped. The mixture was kept at 0 °C for 1 day and 80 °C for 4 days under static conditions. Finally, the template was removed by washing with a mixture of HCl aq. and methanol, and calcination was performed in a box furnace in air at 550 °C for 5 h, with a ramp rate of 1 °C min^{-1}.

To visually study the morphologies of the obtained silica, we used field emission scanning electron microscopy (FESEM).‡ Before taking FESEM images, 10 nm Pt–Pd was covered on the surface of samples. Although the obtained silica combined some nano-sheets, branched silica nanoribbons were identified (Fig. 2 and Supporting information, Fig. S1†). All of these nanoribbons are left-handed twisted with a uniform helical pitch of around 3.0 μm. Generally, these nanoribbons are less than 10 μm in length. Lamellar pore architecture was identified from transmission electron microscope (TEM) images (Fig. 3 and Supporting information, Fig. S2†). This nanostructure is different from the twisted ribbons constructed by many tubes in a single layer.[11] It is very interesting to find that the

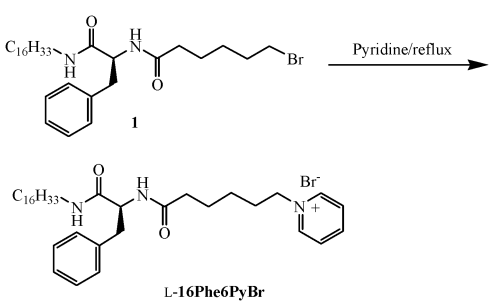

Scheme 1 Synthesis of compound L-**16Phe6PyBr**.

[a] *Key Laboratory of Organic Synthesis of Jiangsu Province, College of Chemistry and Chemical Engineering, Suzhou University, Suzhou 215123, P. R. China. E-mail: ygyang@suda.edu.cn*
[b] *Department of Functional Polymer Science, Faculty of Textile Science and Technology, Shinshu University, Ueda 386-8567, Japan*
† Electronic supplementary information (ESI) available: Synthesis of compound L-**16Phe6PyBr**; FESEM and TEM images; SAXRD pattern. See DOI: 10.1039/b812016a

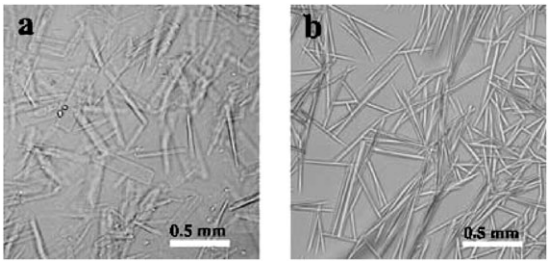

Fig. 1 Optical micrographs of L-**16Phe6PyBr** in pure water (a, 10 mg of L-**16Phe6PyBr** in 1.0 mL of water) and in 1-propanol (b, 10 mg of L-**16Phe6PyBr** in 1.0 mL of 1-propanol).

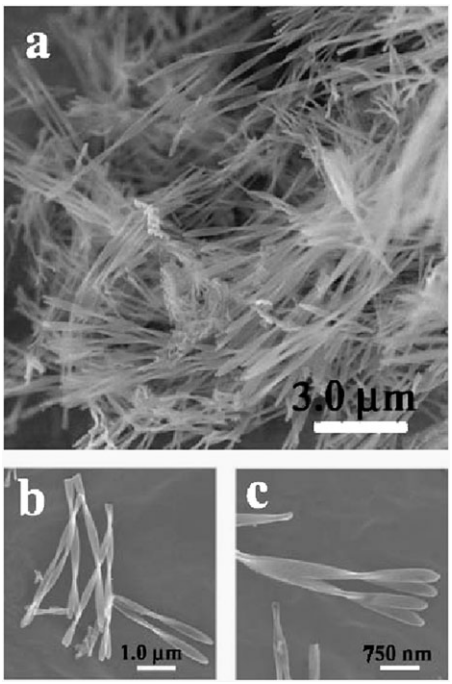

Fig. 2 FESEM (a, b, and c) images of branched mesoporous silica nanoribbons.

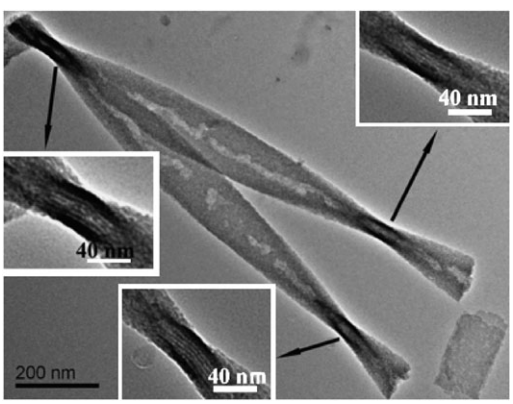

Fig. 3 TEM image of branched mesoporous silica nanoribbons after calcination.

thickness of the trunk and the branch of some ribbons is nearly the same (Fig. 2b and 3). The mesoporous nanoribbons exhibited a nitrogen Brunauer–Emmett–Teller (BET) surface area of 306 m^2 g^{-1} and the Barrett–Joyner–Halenda (BJH) pore-size distribution plot determined from the adsorption branch shows one sharp peak at 4.0 nm (Fig. 4). This lamellar pore architecture shows high thermostability, even this silica was calcined at 550 °C for 5 h. The small-angle X-ray diffraction (SAXRD) pattern shows no sharp peaks (Supporting information, Fig. S3†). Several kinds of helical and coiled mesoporous silica nanostructures have been prepared recently.[11,12] Only broad peaks were identified in SAXRD patterns. For the lamellar mesoporous silica nanoribbons shown here, possibly due to the twisted morphology and the ribbons formed only by several silica layers, no sharp peaks were identified in the SAXRD pattern.

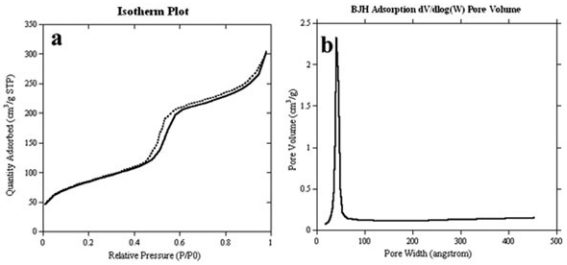

Fig. 4 N_2 adsorption–desorption measurements of left-handedly twisted mesoporous silica nanoribbons. Sorption isotherms (a) and BJH pore-size distribution plot (b) from the adsorption branch.

The mechanism of the formation of the branched mesoporous ribbons was studied using TEM at different reaction times (Fig. 5).[14] Before dropping TEOS, both ribbons and helical bundles were identified (Fig. 5a). After dropping TEOS, dendrimer-like organic self-assemblies were identified at 30 s

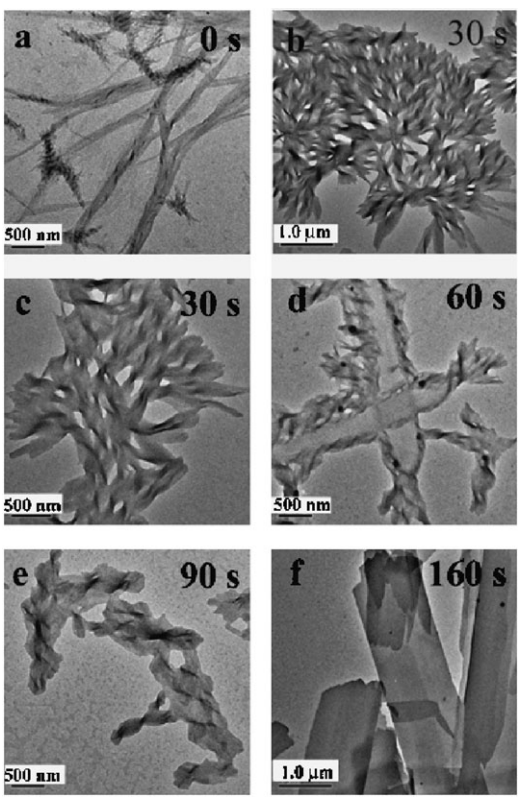

Fig. 5 TEM images of the reaction mixture at different reaction times (a, 0 s; b, 30 s; c, 30 s; d, 60 s; e, 90 s, and f, 160 s).

(Fig. 5b). Each twisted nanoribbon is separated into two twisted nanoribbons (Fig. 5c). Branched nanoribbons were still identified at 90 s, just after stopping stirring (Fig. 5e). These branched nanoribbons organized into non-coiled nanoribbons with increasing stirring time (Fig. 5d and e). The non-coiled nanoribbons started to form at 60 s with self-assembling of twisted nanoribbons (Fig. 5d). Then non-coiled nanoribbons and branched nanoribbons were obtained finally (Fig. 5e and Supporting information, Fig. S4†). Compared with Fig. 5a, c, and d, it was found that the helical pitch of the morphologies increased with increasing reaction time. The branched nanoribbon (Fig. 5b) was the intermediate between the helical bundle (Fig. 5a) and non-coiled nanoribbon (Fig. 5f). Because of the existence of 1-propanol in the reaction mixture, ethanol resulting from the hydrolysis of TEOS should not be the main factor to change the morphologies of the organic self-assemblies from the nanoribbons and helical bundles to the dendrimer-like structure. Thus, the adsorption of silicate anions and silica oligomers should be the main factors controlling this morphology change. After the polycondensation of the silica oligomers on the surface of the branched organic self-assemblies, branched silica nanoribbons were formed. Branched mesoporous silica nanoribbons were obtained by removing the templates. In all, the formation of branched mesoporous silica nanoribbons follows the dynamic template process.[15] The morphologies of organic self-assemblies change during the sol–gel transcription process.

Circular dichroism (CD) and ultra-violet (UV) absorption spectra were taken to study the packing of L-**16Phe6PyBr** molecules (Fig. 6). For the UV absorption, two bands are identified from 240 to 280 nm. The CD sign at 229 nm originates from the carboxy groups. π–π interactions among aromatic rings play an important role in the formation of organic self-assemblies.[16] Two induced CD signs are identified at 258 and 273 nm in the CD spectrum, which originate from the π–π interactions among the phenyl and pyridinium rings, respectively. It seems that the phenyl groups are packing in a right-handed manner. However, the pyridinium rings are packing in a left-handed manner. The interactions of the hydrophobic association of the hydrocarbon chains, hydrogen bonding, π–π interactions among the aromatic rings, and the adsorption of silicate anions and silica oligomers induce the formation of non-coiled nanoribbons. Compared with the other gelators reported previously,[11,12,14] the π–π interaction among the phenyl groups of L-**16Phe6PyBr** is the main factor forming the non-coiled nanoribbons.

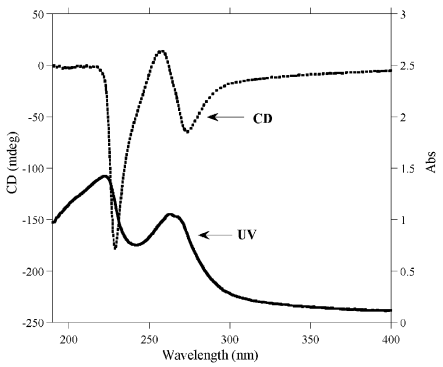

Fig. 6 CD and UV absorption spectra of L-**16Phe6PyBr** viscous aqueous solution (20 mg of L-**16Phe6PyBr** in 1.0 mL of water).

In summary, branched mesoporous silica nanoribbons were fabricated through a dynamic templating process. These branched nanoribbons have a left-handed twist and show high thermostability. They are templated by the intermediates of the organic self-assemblies during the sol–gel transcription process. Based on the mechanism shown here, many other branched nanoparticles have the potential to be prepared, which could be used in electronics and photonics.

This work was partially supported by Jiangsu Provincial Key Laboratory of Organic Chemistry Foundation and Natural Science Foundation of Jiansu Province (No. BK2007047).

Notes and references

‡ TEM images were obtained using a TecnaiG220. FESEM images were taken on a Hitachi S-5000. Specific surface area and pore-size distribution were determined by the BET and BJH methods using a N_2 adsorption isotherm measured by a Gemini V 2380 instrument. The SAXRD pattern was taken on an X'Pert-Pro MPD X-ray diffractometer. CD and UV spectra were taken on an AVIV 410 spectrometer.

1 Y.-S. Ding, X.-F. Shen, S. Gomez, H. Luo, M. Aindow and S. L. Suib, *Adv. Funct. Mater.*, 2006, **16**, 549.
2 J. Zhu, H. Peng, C. C. Chan, K. Jarausch, X. F. Zhang and Y. Cui, *Nano Lett.*, 2007, **7**, 1095.
3 J. Tang and A. P. Alivisatos, *Nano Lett.*, 2006, **6**, 2701.
4 C. L. Nehl, H. Liao and J. H. Hafner, *Nano Lett.*, 2006, **6**, 683.
5 S. H. Yun, J. Z. Wu, A. Dibos, X. Zou and U. O. Karlsson, *Nano Lett.*, 2006, **6**, 385.
6 D. Wei, Y. Liu, L. Cao, L. Fu, X. Li, Y. Wang, G. Yu and D. Zhu, *Nano Lett.*, 2006, **6**, 186.
7 C. Papadopoulos, A. Rakitin, J. Li, A. S. Vedeneev and J. M. Xu, *Phys. Rev. Lett.*, 2000, **85**, 3476.
8 Y. Ono, K. Nakashima, M. Sano, Y. Kanekiyo, K. Inoue, J. Hojo and S. Shinkai, *Chem. Commun.*, 1998, 1477; T. Shimizu, M. Masuda and H. Minamikawa, *Chem. Rev.*, 2005, **105**, 1401; J. H. Jung, Y. Ono and S. Shinkai, *Chem.–Eur. J.*, 2000, **6**, 4552; S. Kobayashi, N. Hamasaki, M. Suzuki, M. Kimura, H. Shirai and K. Hanabusa, *J. Am. Chem. Soc.*, 2002, **124**, 6550; K. Sugiyasu, S. Tamaru, M. Takeuchi, D. Berthier, I. Huc, R. Oda and S. Shinkai, *Chem. Commun.*, 2002, 1212; J. H. Jung, K. Yoshida and T. Shimizu, *Langmuir*, 2002, **18**, 8724; Y. Yang, M. Suzuki, S. Owa, H. Shirai and K. Hanabusa, *J. Mater. Chem.*, 2006, **16**, 1644; Y. Yang, H. Fukui, M. Suzuki, H. Shirai and K. Hanabusa, *Bull. Chem. Soc. Jpn.*, 2005, **78**, 2069.
9 J. J. E. Moreau, L. Vellutini, M. Wong Chi Man and C. Bied, *J. Am. Chem. Soc.*, 2001, **123**, 1509; Y. Yang, M. Nakazawa, M. Suzuki, M. Kimura, H. Shirai and K. Hanabusa, *Chem. Mater.*, 2004, **16**, 3791.
10 J. H. Jung, Y. Ono, K. Hanabusa and S. Shinkai, *J. Am. Chem. Soc.*, 2000, **122**, 5008.
11 Y. Yang, M. Suzuki, S. Owa, H. Shirai and K. Hanabusa, *J. Am. Chem. Soc.*, 2007, **129**, 581.
12 Y. Yang, M. Suzuki, S. Owa, H. Shirai and K. Hanabusa, *Chem. Commun.*, 2005, 4462.
13 A. M. Seddon, H. M. Patel, S. L. Burkett and S. Mann, *Angew. Chem., Int. Ed.*, 2002, **41**, 2988.
14 X. Wan, X. Pei, H. Zhao, Y. Chen, Y. Guo, B. Li, K. Hanabusa and Y. Yang, *Nanotechnology*, 2008, **19**, 315602; Y. Chen, Y. Guo, H. Zhao, L. Bi, X. Pei, B. Li and Y. Yang, *Nanotechnology*, 2008, **19**, 355603.
15 E. Pouget, E. Dujardin, A. Cavalier, A. Moreac, C. Valéry, V. Marchi-Artzner, T. Weiss, A. Renault, M. Paternostre and F. Artzner, *Nat. Mater.*, 2007, **6**, 434.
16 M. Llusar, C. Roux, J. L. Pozzo and C. Sanchez, *J. Mater. Chem.*, 2003, **13**, 442; M. Llusar, G. Monrós, C. Roux, J. L. Pozzo and C. Sanchez, *J. Mater. Chem.*, 2003, **13**, 2505.

